

Published in final edited form as:

J Neurosci Methods. 2014 July 30; 232: 165–172. doi:10.1016/j.jneumeth.2014.05.013.

An *in vitro* Blood-brain barrier model combining shear stress and endothelial cell/astrocyte co-culture

Yukio Takeshita¹, Birgit Obermeier¹, Anne Cotleur¹, Yasuteru Sano², Takashi Kanda², and Richard M. Ransohoff¹

¹Neuroinflammation Research Center, Department of Neuroscience, Lerner Research Institute, Cleveland Clinic

²Department of Neurology and Clinical Neuroscience, Yamaguchi University Graduate School of Medicine, Ube, Yamaguchi Japan

Abstract

Background—In vitro blood-brain barrier (BBB) models can be useful for understanding leukocyte-endothelial interactions at this unique vascular-tissue interface. Desirable features of such a model include shear stress, non-transformed cells and co-cultures of brain microvascular endothelial cells with astrocytes. Recovery of transmigrated leukocytes for further analysis is also appealing.

New methods—We report an in vitro BBB model for leukocyte transmigration incorporating shear stress with co-culture of conditionally immortalized human endothelial cell line (hBMVEC) and human astrocyte cell line (hAST). Transmigrated leukocytes can be recovered for comparison with input and non-transmigrated cells.

Result—hBMVEC and hAST exhibited physiological and morphological BBB properties when cocultured back-to-back on membranes. In particular, astrocyte processes protruded through 3µm membrane pores, terminating in close proximity to the hBMVEC with a morphology reminiscent of end-feet. Co-culture with hAST also decreased the permeability of hBMVEC. In our model, astrocytes promoted transendothelial leukocyte transmigration.

Comparison with Existing Method—This model offers the opportunity to evaluate whether BBB properties and leukocyte transmigration across cytokine-activated hBMVEC are influenced by human astrocytes.

Conclusions—We present a model for leukocyte transmigration incorporating shear stress with coculture of hBMVEC and hAST. We demonstrated that hAST promoted leukocyte transmigration and also increased certain barrier functions of hBMVEC. This model provides

Corresponding to: Richard M. Ransohoff, Neuroinflammation Research Center, Department of Neurosciences, Lerner Research Institute, Cleveland Clinic, Mail Code NC30, 9500 Euclid Avenue, Cleveland, Ohio 44195, USA. Tel.: +1 216 444 0627, Fax: +1 216 444 7927, ransohr@ccf.org.

The author has no conflicts of interest to declare.

Publisher's Disclaimer: This is a PDF file of an unedited manuscript that has been accepted for publication. As a service to our customers we are providing this early version of the manuscript. The manuscript will undergo copyediting, typesetting, and review of the resulting proof before it is published in its final form. Please note that during the production process errors may be discovered which could affect the content, and all legal disclaimers that apply to the journal pertain.

reproducible assays for leukocyte transmigration with robust results, which will enable further defining the relationships among leukocytes and the cellular elements of the BBB.

Keywords

blood-brain barrier; human endothelial cell line; human astrocyte cell line; in vitro model; shear forces; leukocyte transmigration; co-culture; migration assay

1. Introduction

The blood-brain barrier (BBB) is the brain-specific capillary barrier that is critical to maintaining ionic and chemical homeostasis of the central nervous system (CNS). The BBB limits the entry of inflammatory hematogenous cells and plasma proteins into the CNS. In pathological conditions inflammatory cells may enter the CNS due to activation of the BBB and these cells can mediate tissue injury or host defense. The invasion of inflammatory cells across cerebrovascular endothelium is involved in neurological disorders such as multiple sclerosis (Holman et al., 2011), encephalomyelitis (Furtado et al., 2006), neuromyelitis optica (Ransohoff, 2012), and stroke (Petty and Lo, 2002). Leukocyte-endothelial interactions at the BBB often play a key role in the pathogenesis of neurological disorders (Man et al., 2007). Some mechanistic aspects of leukocyte transmigration still remain largely unknown at the cellular and molecular level.

Previously, we developed a flow-based monoculture system that allows the transendothelial migration of inflammatory cells with the addition of chemokines (Man et al., 2012). This model provided a three-dimensional (3D), controllable environment where vascular endothelial cells can be exposed to physiological levels of flow and chemokines.

In the present model, we aimed to incorporate four properties as helpful for an *in vitro* BBB model (Takeshita and Ransohoff, 2013). These attributes were:

1. Inclusion of human cells that will maintain both physiological and morphological BBB properties *in vitro* and provide species-compatible trafficking determinants for human leukocytes;
2. Endothelial cells co-cultured with other BBB cells such as astrocytes;
3. Incorporation of shear forces;
4. Ability to recover leukocytes for analysis after transmigration.

In order to initiate an *in vitro* BBB model with these four properties, we utilized the temperature sensitive Simian virus-40 large T antigen (ts-SV40-LT) transfected hBMVEC (Sano et al., 2010) and hAST (Shimizu et al., 2013; Haruki et al., 2013). We co-cultured hBMVEC and hAST in a 3D Flow Chamber (C.B.S. Scientific Company, San Diego, CA), which enabled us to evaluate leukocyte interaction with, and transmigration across the endothelium under shear forces. Using this model, we evaluated the effect of hAST on hBMVEC BBB properties and leukocyte transmigration across the hBMVEC.

2. Material and method

2.1. Human subjects

Healthy volunteers between 20 and 50 years old were recruited. The Cleveland Clinic Institutional Review Board approved all study protocols, and signed informed consents were obtained from all blood donors. Subjects were not experiencing systemic infection or taking nonsteroidal anti-inflammatory drugs (NSAIDs) at the time of phlebotomy.

2.2. Cell culture

hBMVEC are adult human brain microvascular endothelial cells transfected and immortalized with plasmid expressing ts-SV40-LT as previously described (Sano et al., 2010). hBMVEC were grown in media (EGM-2 Bulletkit, Lonza, Basel Switzerland) supplemented with 20 % FBS, 100 U/ml penicillin (Sigma Aldrich, St. Louis, MO) and 100 µg/ml streptomycin (Sigma Aldrich).

hAST are clonal adult human astrocyte cells transfected and immortalized with plasmid containing ts-SV40-LT as previously described (Shimizu et al., 2013, Haruki et al., 2013). hAST were grown in Astrocyte media (ScienCell Research Laboratories, Carlsbad, CA) containing 10 % heat-inactivated fetal bovine serum and 100 µg/ml streptomycin (Sigma Aldrich). Astrocyte media was used as co-culture medium.

All cells were maintained in 5 % carbon dioxide at 33°C. All analyses were performed one or two days after the temperature shift from 33 °C to 37 °C.

2.3. Immunocytochemistry

Zo-1, Occludin, Claudin-5, von Willebrand factor (vWF), and Glial fibrillary acidic protein (GFAP), ICAM1 and GLUT-1 were detected by indirect immunocytochemistry on confluent hBMVEC or hAST as previously described (Man et al., 2008). Polyclonal rabbit anti-human Zo-1 antibodies (Zymed Laboratories, San Francisco CA: Catalog #402300), anti-human GLUT-1 antibodies (Novus: #NBI10-31113) and anti-human Occludin antibodies (Zymed Laboratories: #71-1500), anti-human vWF (DAKO, Carpinteria: #A008229-5), monoclonal mouse anti-human Claudin-5 antibody (Zymed Laboratories: #35-2500), anti-human GFAP (COVANCE, Madison, WI: #SM1-26R), anti-human ICAM1 antibody (Santa Cruz Biotechnology, Santa Cruz, CA: #sc-18908) and Alexa Fluor®488 goat anti-rabbit IgG (Invitrogen, Carlsbad, CA: #A-11008) and anti-mouse IgG (Invitrogen: #A-11001) were used. Slides were viewed using a Leica SP5 laser scanning confocal microscope (Leica Microsystems, Exton, PA).

2.4. Permeability

hBMVEC or hAST were cultured to confluence on 24-well collagen-coated Transwell™ tissue culture inserts (3 µM pore size) (Corning Inc., Corning, NY) in 37°C. Solute paracellular permeability was assessed using 10 kDa Dextran-conjugated FITC (1 mg/ml)(Sigma Aldrich) and fluorescent recovery in the lower chamber was measured after 20, 60, and 120 minutes using a SpectraMax M2e microplate reader (Molecular Devices, Sunnyvale, CA).

Apparent permeability coefficients (P_{app} ; cm/min) was calculated using the following formula:

$$P_{app} = V(dc/dt) / AC_0$$

dc/dt = dextran flux across the membrane. $V(\text{cm}^3)$ = volume in the receiver side.

$A (\text{cm}^2)$ = surface area of insert. $C_0 (\text{mM})$ = initial concentration in the donor compartment.

2.5. PBMC isolation

Peripheral blood mononuclear cells (PBMCs) were isolated from fresh heparinized blood of healthy subjects by density centrifugation with Lymphocyte Separation Medium (Mediatech, Herndon, VA) as previously described (Mahad et al., 2006). PBMCs were resuspended at 10×10^6 cells in 30 ml TEM buffer (RPMI 1640 without phenol red + 1% bovine serum albumin + 25mM Hepes) for transmigration assays and assayed within two hours of phlebotomy. PBMC were stained with Calcein AM (Invitrogen) prior to perfusion into the chamber following the manufacturer's protocol.

2.6. 3D Flow system and transmigration assay

3D flow chamber Device (C.B.S. Scientific company) was used for transmigration assay. 3D Flow pump, 3D Flow chamber, and 3D flow membranes constitute this system (Fig. 5A and B). The pump delivers programmable shear flow to up to eight flow devices. It covers a wide shear range (0.1–200 dyne/cm²). 3D Flow chamber (depth: 30 mm, width: 70 mm, height: 8 mm) has three discrete reservoirs that fit the 3D flow membrane completely. The 3D flow membrane is 8 mm in diameter and made of Track-etched polycarbonate with 3 μm pores. These membranes were coated with rat-tail collagen I solution (50 $\mu\text{g}/\text{ml}$) (BD Bioscience, San Diego, CA) and placed in a 12 well plate. 5×10^4 hAST were seeded on the abluminal side of the membrane, and after one hour incubation in 33 °C, the membrane was flipped gently with tweezers. 10×10^4 hBMVEC were seeded on the luminal side and co-cultured in Astrocyte media for two days in 33 C°, at which time membrane cultures were incubated for one day at 37°C. Then cells were activated with TNF-alpha (5 U/ml) (R and D systems, Minneapolis, MN) and IFN-gamma (20 U/ml) (R and D systems) for 24 hours at 37°C in Astrocyte media. CXCL12 (50 ng/ml) (R and D systems) was dispensed on the apical aspect of hBMVEC and incubated for 15 minutes at 37°C. CCL2 (25 ng/ml) (R and D systems) was loaded in the bottom wells of 3D Flow chamber (Fig. 5A). The membrane was transferred to this chamber gently. 10×10^6 PBMC (total cells per assays) in 30ml TEM (kept warm in a 37°C water bath), were perfused via peristaltic pump through the chamber at a final concentration of 333,000 cells/ml and at a shear stress of 1.5 dyne/cm² resulting in a total assay time of 60 minutes (Fig. 5B). All chambers were set on a 37°C slide warmer. After PBMC perfusion, the chamber was flushed for five minutes with PBS to remove loose cells, maintaining the same shear stress as in the assay. Migrated PBMCs were recovered from the bottom chamber. Cells that attached to the abluminal side of the membrane and the bottom chamber were removed by a quick rinse with 0.5mM EDTA. The migrated cells

were enumerated by a hemocytometer, then normalized to migrated cell numbers determined in transmigration assays using non activated hBMVEC/hAST.

2.7. Phenotyping of PBMC

Input and migrated cells were phenotyped by flow cytometry. After collection, cells were fixed for 10min in 1%PFA at room temperature, washed in PBS+0.1mM EDTA, followed by blocking in mouse IgG. Cells were stained with anti-human CD45 efluor450 and CD8a APC-efluor780 (eBiosciences, San Diego, CA), CD3Alexa Fluor 647 and CD14 BV605 (Biolegend, San Diego, CA), CD19 BV711 CD4 PE-CF594 (BD Biosciences), and CD16PE (R&D Systems). Data was acquired on a BD LSRFortessa SORP flow cytometer running Diva6, and analyzed in Flowjo 9.7.5 (Treestar, Ashland, OR).

2.8. Construction of 3D cell image on the membrane

5×10^4 hAST were seeded on the abluminal side of the membrane and cultured for 2 days at 33°C. They were stained with Cyto-ID™ Red (Enzo Life Sciences, Farmingdale, NY), following manufactures instruction. After the membrane was flipped, 10×10^4 hBMVEC, which were stained with CellTracker™ Green (Invitrogen), were seeded on the luminal side and co-cultured in Astrocyte media for two days in 33 C°. Then, the co-cultured cells were incubated for two more days at 37°C. Membranes were washed with PBS, mounted on slides, and coverslipped before being visualized on the confocal microscope. 3D Images were generated by Fiji software (NIH).

2.9. Electron Microscopy

Co-cultured cells on the membrane were fixed in 4 % Paraformaldehyde/2.5 % Glutaraldehyde in 0.1 M sodium cacodylate buffer for 5 minutes at 37 °C followed overnight at 5 °C. Samples were exposed to 1% osmium tetroxide solution for 1 hour. After dehydrating through a graded series of ethanol, they were embedded in Eponresin. Ultra-thin sections were cut with EM UC7 Ultramicrotome (Leica Microsystems GmbH), then stained with uranyl acetate for observation by TEM with a FEI Tecnai G2 Spirit BioTWIN (FEI, Hillsboro, OR).

2.10. Data analysis

One-way analysis of variable (ANOVA), followed by Tukey-Kramer multiple comparison procedure, was used for statistical analysis. Values of *P* >0.05 were considered significant. All values are expressed as the mean ± SEM (n=6 for permeability and n=6 for migration assay).

Result

3.1. Properties of conditionally immortalized human endothelial cells (hBMVEC)

Properties of hBMVEC have been previously reported (Sano et al., 2010). At 33°C, ts-SV40-LT is stable, leading to continuous cell proliferation. At 37°C ts-SV40-LT is unstable, and the cells exhibit growth arrest and differentiate. hBMVEC exhibited robust proliferation at 33°C. Two days after the temperature shift from 33°C to 37°C, the cell growth was arrested (Fig. 1A). Differentiated hBMVEC in 37°C show a spindle-shaped morphology

resembling primary endothelial cell culture (Fig. 1B). They express vWF, a lineage marker for endothelial cells (Fig. 1C). Zo-1, Claudin-5 and Occludin, representative tight junction molecules, were detected at cell-to-cell boundaries (Fig. 1D–F).

3.2. Properties of conditional immortalized human astrocytes (hAST)

Properties of hASTs have been previously reported (Shimizu et al., 2013, Haruki et al., 2013). hAST proliferated favorably at 33°C. When hAST were cultured at 37°C, their growth rate was lower than at 33°C (Fig. 2A). Differentiated hAST in 37°C were polygonal with numerous processes (Fig. 2B). hAST expressed GFAP, an astrocyte lineage marker (Fig. 2C).

3.3. hBMVEC and hAST co-cultures on membranes

In order to clarify the morphology of hBMVEC and hAST on membranes, 3D images of co-cultured cells were constructed from stacked files. hBMVECs, stained with Cell Tracker Green, were cultured confluent on the “luminal” side of the membrane (Fig. 3A), but not cultured on the abluminal side (C). hAST, stained with CytoID Red, were grown on the “abluminal” side (Fig. 3D). Processes of hAST were detected on luminal side (Fig. 3B). In a 3D picture of co-cultured cells, some hAST processes resembling endfeet were observed protruding through the membrane pores towards the endothelium (arrow), some of which were in close proximity to hBMVEC (Fig. 3E). We performed EM studies to delineate glial filipodia, and found that A hAST extended process into membrane pore (Fig. 3F).

3.4. The effect of astrocytes and cytokines on hBMVEC function

In order to evaluate the effect of astrocytes and cytokines (TNF-alpha and IFN-gamma) on the integrity of hBMVEC, we examined the paracellular permeability of dextran 10K across our BBB model. When cells were activated by cytokines, the apparent permeability coefficients (P_{app} ; cm/min) in activated cells, was significantly higher than non-activated cells regardless of co-culture (Fig. 4A). The P_{app} of hBMVEC/hAST was significantly lower than mono-cultured hBMVEC, regardless cytokines activation. The P_{app} of mono-cultured hAST, even if they were activated, was more than 10 times that of hBMVEC and was almost same as that of membrane without cells (supplemental 1). These findings indicated that cytokine activation decreased barrier function and that co-culturing with astrocytes increased barrier function of endothelial cells.

In order to evaluate the effect of astrocytes and cytokines in endothelial cells for barrier function, transporter, and leukocyte-endothelial interaction at the BBB, the expressions of claudin-5, GLUT-1 and ICAM1 were compared in activated and nonactivated hBMVEC/hAST and hBMVEC. The expression level of Claudin-5, which is one of the most important key tight junction molecules, were decreased when hBMVEC were mono-cultured and activated by cytokines (Fig 4B upper panels). GLUT-1, which is a representative transporter molecule, increased their expression level when hBMVEC were co-cultured with astrocytes nevertheless the activation of cytokines (Fig 4B middle panels). ICAM-1, which is the key adhesion molecules for leukocyte transmigration, increased its expression when hBMVEC were activated by cytokines when co-cultured with astrocytes (Fig 4B lower panels).

3.5. Astrocytes affect leukocyte transmigration at the BBB *in vitro*

We examined leukocyte transmigration using this BBB model. In this model, a co-cultured membrane was sandwiched in a 3D Flow chamber (Fig. 5A). PBMC were perfused through the chamber by a peristaltic pump after connecting the tube (Fig. 5B). We confirmed that Claudin-5 expression was stable before and after shear-force imposition and transmigration (Fig. 5C). In order to evaluate whether the confluence of the hBMVECs controlled PBMC transmigration, we compared the total migrated cell number in subconfluent hBMVEC and confluent hBMVEC monolayer. The total migrated PBMC in confluent hBMVEC were significantly higher than subconfluent hBMVEC (Fig. 5D). Relative migration index was significantly higher in co-culture than in monoculture in dependent of cytokine activation (Fig. 5E). In phenotyping results, activation by cytokines and co-culture with hAST increased CD14+, CD3+, CD19+, CD4+, and CD8+ cells (Fig. 5F–J). Total cell number of migrated leukocytes varied among donors (supplemental 2). These data indicate that co-culture with hAST and cytokine activation, promote leukocyte (monocyte, T cells, and B cells) transmigration across endothelial cells and that this model will enable us to define interactions between leukocytes and the BBB endothelium when co-cultured with hAST.

4. Discussion

We developed a new BBB model that incorporates hBMVEC/hAST co-culture and allows further investigation of leukocyte transmigration assays under flow. This model showed that astrocytes promote transendothelial leukocyte transmigration, and modulate the barrier properties of endothelial cells. Moreover, our novel BBB model offers the opportunity to evaluate the effect of cytokines on BBB integrity and to examine how chemokines regulate leukocyte transmigration in the presence of astrocytes.

The limited availability of primary human endothelial cells and astrocytes, coupled with the difficulty in maintaining these cells *in vitro* in a co-culture system that exhibits high BBB properties, is a challenge not yet overcome (Takeshita and Ransohoff, 2013). Using conditionally immortalized culture systems (such as cells transfected with ts-SV40-LT) offers the opportunity to overcome these challenges. At 37°C, hBMVEC and hAST differentiate into mature cells and retain physiological and morphological properties indicative of BBB attributes. As these human conditionally immortalized cell lines are easier to culture compared to primary human cells, they represent a useful material for *in vitro* BBB experiments.

We demonstrated that abluminal astrocyte processes protruded through membrane pores and contact, luminal hBMVEC. Astrocyte endfeet are the cell components in closest proximity to brain capillary endothelial cells (Choi and Zheng, 2009). Astrocytic endfeet ensheath 99% of the surface of brain microvessels, where their endfoot processes are separated only by a thin basal membrane (Hawkins and Davis, 2005). For this reason, it is suggested that our co-culture system allows communication between endothelial cells and astrocytes.

Here we showed that hAST increased the barrier function of hBMVEC and augmented leukocyte transmigration across hBMVEC. Astrocytes secrete important regulatory factors for endothelium (Mi et al., 2001) such as transforming growth factor beta (TGF-beta)

(Dohgu et al., 2005), glial-derived neurotrophic factor (GDNF) (Igarashi et al., 1999), the fibroblast growth factor (FGF) (Reuss et al., 2003), and vascular endothelial growth factor (VEGF) (Wang et al, 2001; Argaw et al., 2012). Astrocytes also serve as one of the major sources of chemokines that can promote transendothelial leukocyte migration across the BBB (Ransohoff et al., 1993; Falsiq et al., 2006; Kang et al., 2010). As astrocytes can provide these secreted factors to endothelial cells, the current predominant view is that astrocytes regulate various aspects of BBB physiology with secreted factors and influence BBB features including solute permeability and tight junction protein expression and subcellular distribution (Alvarez et al., 2011).

5. Conclusion

We established an *in vitro* BBB model that incorporates co-culturing hBMVEC and hAST, maintains BBB properties, and allows leukocyte transmigration assay under flow. Using this model, we demonstrated that hAST could help leukocyte transmigration and increase BBB function of hBMVEC. We also showed that this model incorporated four important properties necessary for a useful *in vitro* BBB model. This model provides reproducible assays with robust results to define anatomical and functional relationships among leukocytes and the cellular elements of the BBB, represented by endothelial cells and astrocytes. Pathological circumstances can be simulated, and thereby CNS diseases that are associated with an impaired BBB can be studied. Moreover, the effects of various therapeutics on BBB integrity can be examined, altogether allowing a wide spectrum of applications.

Supplementary Material

Refer to Web version on PubMed Central for supplementary material.

Acknowledgments

This study was supported by the Guthy Jackson Charitable Foundation and by the National Institutes of Health (K24NS51400, R21NS78420, and P50NS38667, Project 1 to R.M.R.).

References

- Alvarez JI, Cayrol R, et al. Disruption of central nervous system barriers in multiple sclerosis. *Biochim Biophys Acta*. 2011; 1812 (2):252. [PubMed: 20619340]
- Argaw AT, Asp L, et al. Astrocyte-derived VEGF-A drives blood-brain barrier disruption in CNS inflammatory disease. *J Clin Invest*. 2012; 122 (7):2454. [PubMed: 22653056]
- Choi BS, Zheng W. Copper transport to the brain by the blood-brain barrier and blood-CSF barrier. *Brain Res*. 2009; 1248 (12):14. [PubMed: 19014916]
- Dohgu S, Takata F, et al. Brain pericytes contribute to the induction and up-regulation of blood-brain barrier functions through transforming growth factor-beta production. *Brain Res*. 2005; 1038 (2): 208. [PubMed: 15757636]
- Falsig J, Pörzgen P, et al. The inflammatory transcriptome of reactive murine astrocytes and implications for their innate immune function. *J Neurochem*. 2006; 96 (3):893. [PubMed: 16405499]
- Furtado GC, Pina B, et al. A novel model of demyelinating encephalomyelitis induced by monocytes and dendritic cells. *J Immunol*. 2006; 177 (10):6871. [PubMed: 17082601]

- Haruki H, Sano Y, et al. NMO-sera down-regulate AQP4 in human astrocyte and induce cytotoxicity independent of complement. *J Neurol Sci.* 2013; 331 (1–2):136. [PubMed: 23809190]
- Hawkins BT, Davis TP. The blood-brain barrier/neurovascular unit in health and disease. *Pharmacol Rev.* 2005; 57 (2):173. [PubMed: 15914466]
- Holman DW, Klein RS, et al. The blood-brain barrier, chemokines and multiple sclerosis. *Biochim Biophys Acta.* 2011; 1812 (2):220. [PubMed: 20692338]
- Igarashi Y, Utsumi H, et al. Glial cell line-derived neurotrophic factor induces barrier function of endothelial cells forming the blood-brain barrier. *Biochem Biophys Res Commun.* 1999; 261 (1): 108. [PubMed: 10405331]
- Kang Z, Altuntas CZ, et al. Astrocyte-restricted ablation of interleukin- 17-induced Act1-mediated signaling ameliorates autoimmune encephalomyelitis. *Immunity.* 2010; 32 (3):414. [PubMed: 20303295]
- Lahtz F, Piali L, et al. Chemokines in viral meningitis: chemotactic cerebrospinal fluid factors include MCP-1 and IP-10 for monocytes and activate T lymphocytes. *Eur J Immunol.* 1997; 27 (10):2484. [PubMed: 9368600]
- Mahad D, Callahan MK, et al. Modulating CCR2 and CCL2 at the blood-brain barrier: relevance for multiple sclerosis pathogenesis. *Brain.* 2006; 129 (1):212. [PubMed: 16230319]
- Man S, Ubogu EE, et al. Inflammatory cell migration into the central nervous system: a few new twists on an old tale. *Brain Pathol.* 2007; 17 (2):243. [PubMed: 17388955]
- Man S, Ubogu EE, et al. Human brain microvascular endothelial cells and umbilical vein endothelial cells differentially facilitate leukocyte recruitment and utilize chemokines for T cell migration. *Clin Dev Immunol.* 2008; 2008 (2008):384982. [PubMed: 18320011]
- Man S, Tucky B, et al. CXCL12-induced monocyte-endothelial interactions promote lymphocyte transmigration across an *in vitro* blood-brain barrier. *Sci Transl Med.* 2012; 4 (119):119.
- Mi H, Haeberle H, et al. Induction of astrocyte differentiation by endothelial cells. *J Neurosci.* 2001; 21 (5):1538. [PubMed: 11222644]
- Petty MA, Lo EH. Junctional complexes of the blood-brain barrier: permeability changes in neuroinflammation. *Prog Neurobiol.* 2002; 68 (5):311. [PubMed: 12531232]
- Ransohoff RM, Hamilton TA, et al. Astrocyte expression of mRNA encoding cytokines IP-10 and JE/MCP-1 in experimental autoimmune encephalomyelitis. *FABEB J.* 1993; 7 (6):592.
- Ransohoff RM. Illuminating neuromyelitis optica pathogenesis. *Proc Natl Acad Sci USA.* 2012; 109 (4):1001. [PubMed: 22308524]
- Reuss B, Dono R, et al. Functions of fibroblast growth factor (FGF)-2 and FGF-5 in astroglial differentiation and blood-brain barrier permeability: evidence from mouse mutants. *J Neurosci.* 2003; 23 (16):6404. [PubMed: 12878680]
- Sano Y, Shimizu F, et al. Establishment of a new conditionally immortalized human brain microvascular endothelial cell line retaining an *in vivo* blood -brain barrier function. *J Cell Physiol.* 2010; 225 (2):519. [PubMed: 20458752]
- Shimizu F, Sano Y, et al. Advanced glycation end-products disrupt the blood-brain barrier by stimulating the release of transforming growth factor- β by pericytes and vascular endothelial growth factor and matrix metalloproteinase-2 by endothelial cells *in vitro*. *Neurobiol Aging.* 2013; 34 (7):1902. [PubMed: 23428182]
- Takeshita Y, Ransohoff RM. Inflammatory cell trafficking across the blood-brain barrier: chemokine regulation and *in vitro* models. *Immunol Rev.* 2012; 248 (1):228. [PubMed: 22725965]
- Wang W, Dentler WL, et al. VEGF increases BMEC monolayer permeability by affecting occludin expression and tight junction assembly. *Am J Physiol Heart Circ Physiol.* 2001; 280 (1):434.

- We established the flow based BBB model incorporating endothelium and astrocyte.
- Astrocyte could help leukocyte migration and increase BBB function of endothelium.
- This model will enable defining the relationships among leukocytes and BBB.

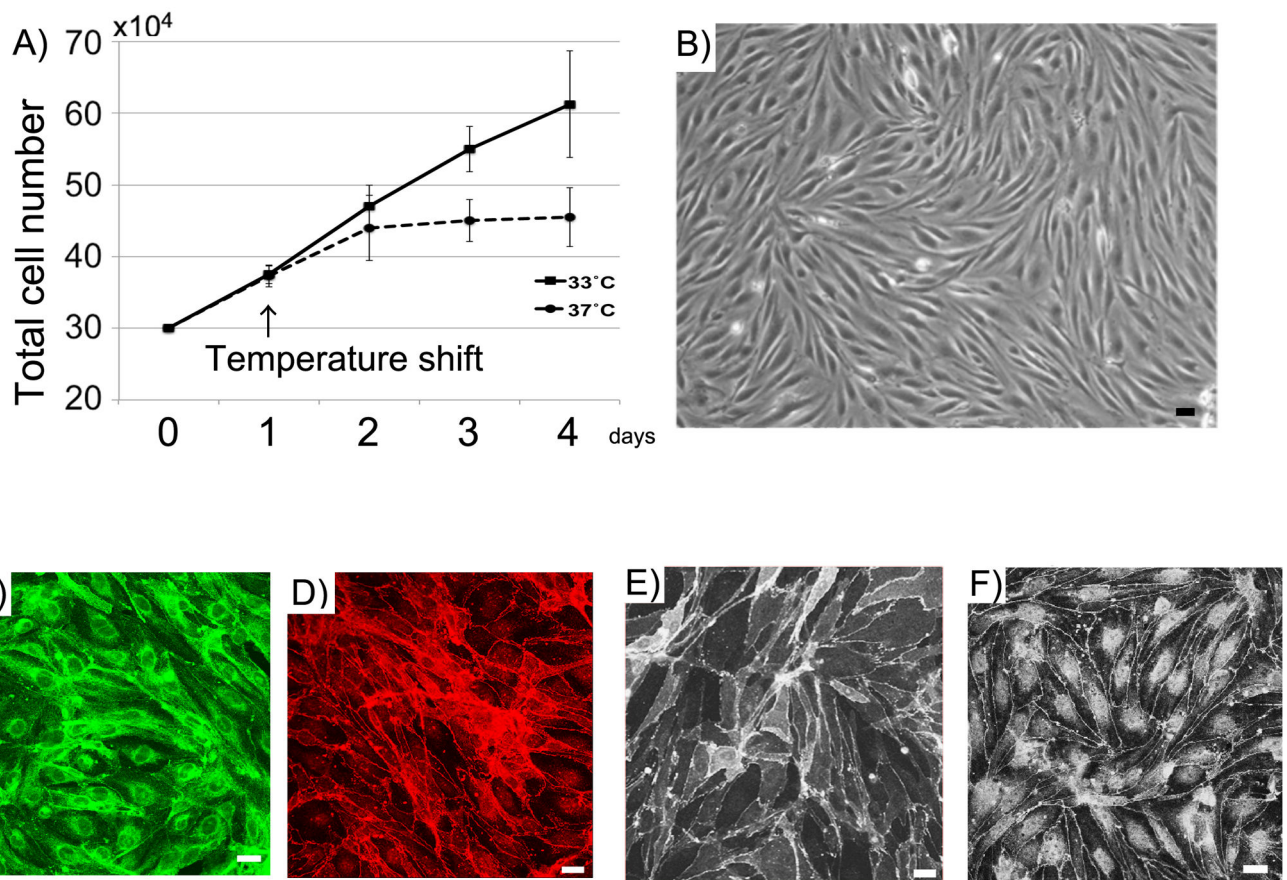


Fig. 1.

Properties of hBMVEC. (A) Comparison of growth in 33°C and 37°C. 30x10⁴ hBMVEC were seeded on 6 well plate. After culturing for one day at 33°C, they were cultured at 33°C or 37°C. Cells were trypsinized and counted using a hemacytometer. Data are mean ± SEM with n=4 replicates. (B) Morphology of hBMVEC. hBMVEC were cultured on 6 well plate at 37°C. (C–F) Confocal single images of hBMVEC stained for vWF (C), Zo-1 (D), Occludin (E), and Claudin-5 (F). Scale bar represents 10 μm.

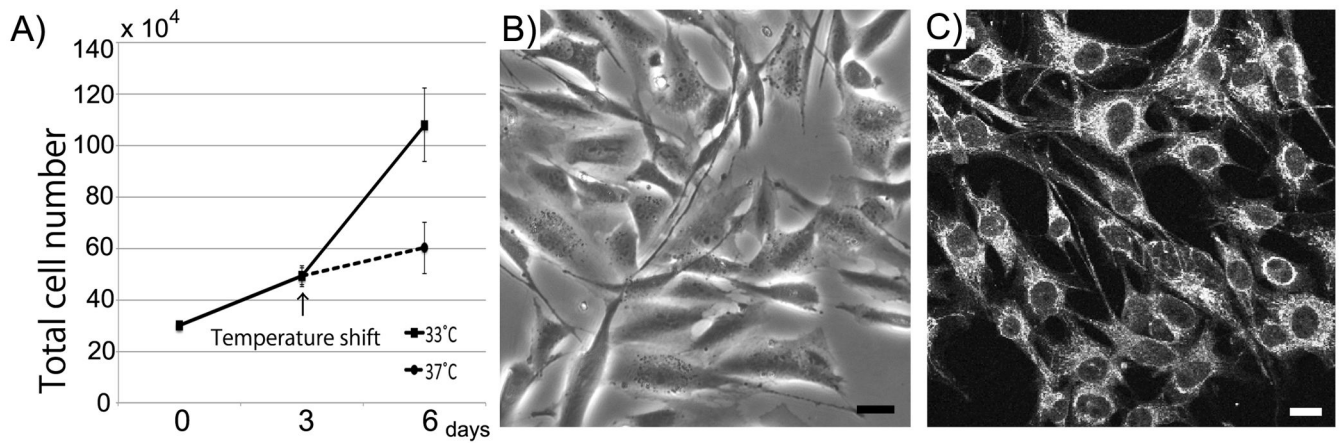


Fig. 2.

Properties of hAST. (A) Comparison of growth in 33°C and 37°C. 30×10^4 hBMVEC were seeded on 6 well plate. After culturing for one day at 33°C, they were cultured at 33°C or 37°C. Cells were trypsinized and counted using a hemacytometer. Data are mean \pm SEM with $n=4$ replicates. (B) Morphology of hAST. hAST were cultured on 6 well plate at 37°C. (C) Confocal single image of hAST stained for GFAP. Scale bar represents 10 μ m.

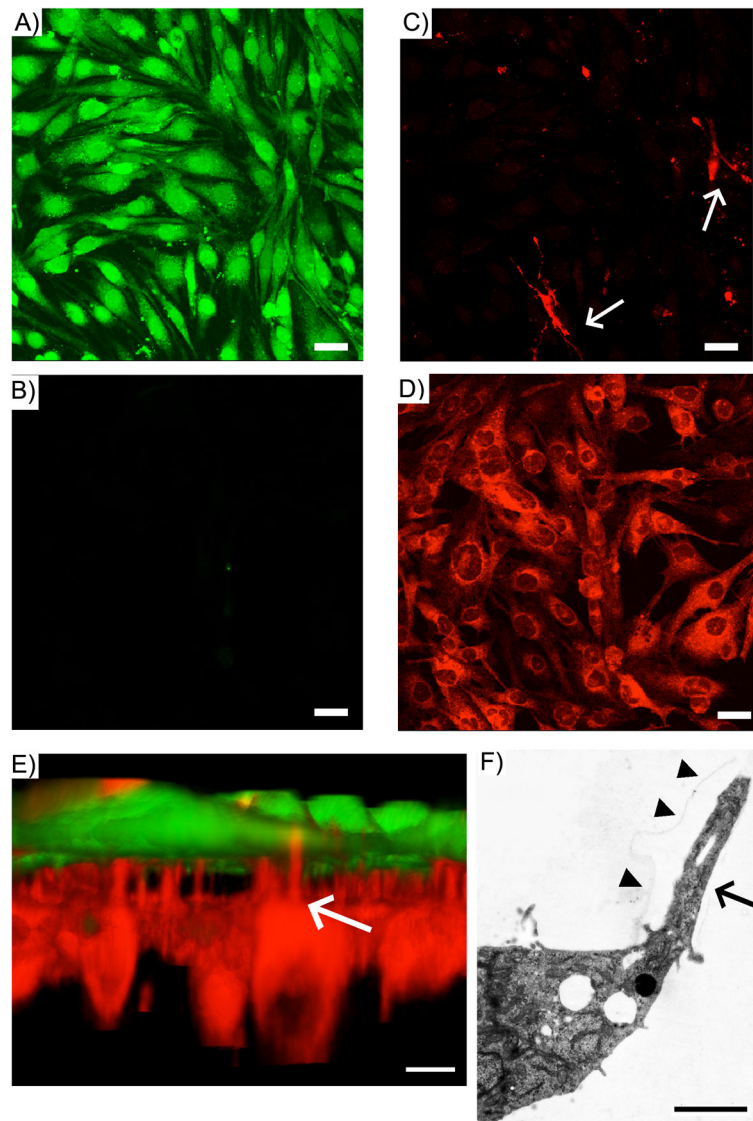


Fig. 3. 3D structure of hBMVEC/hAST co-cultures on membranes. (A–D) morphology of co-cultured cells on the membrane. hBMVEC were stained with CellTracker™ Green. hAST were stained with Cyto-ID™ Red. Stack file was constructed from hBMVEC layer to hAST layer; (A) hBMVEC; luminal side (B) hBMVEC; abluminal side (C) hAST; luminal side (D) hAST; abluminal side. (E) 3 D reconstruction of co-cultured cells. This picture was generated from stack file s. Scale bar represents 10 μm. Arrows; hAST processes (F) EM structure of hAST process. Arrow heads; the border of a membrane pore. Scale bar represents 2 μm.

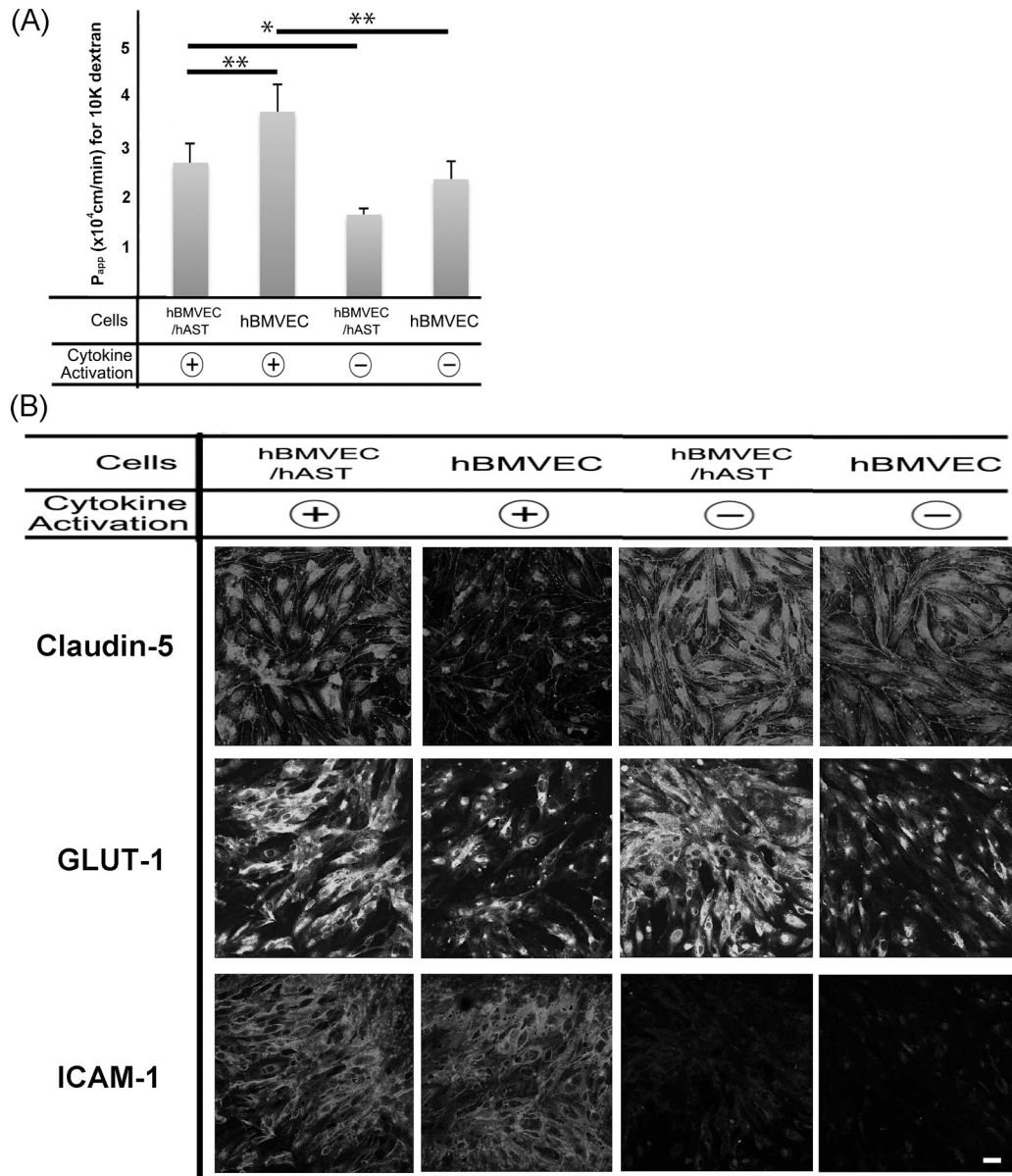


Fig. 4. Effect of astrocytes and cytokines on hBMVEC function (A) Effect of hAST and cytokines on solute permeability of hBMVEC. Comparison of dextran 10K permeability in hBMVEC/hAST co-culture and hBMVEC. Cells were activated with TNF-alpha (5 U/ml) and IFN-gamma (20 U/ml) for 24 hours. * P bold > 0.01, ** P < 0.05. (B) Effect of astrocytes and cytokines in endothelial cells for barrier function, transporter, and leukocyte-endothelial interaction at the BBB. Claudin-5, GLUT-1, and ICAM-1 were detected in activated or nonactivated hBMVEC/hAST and hBMVEC. Claudin-5; upper panel, GLUT-1; middle panel, and ICAM-1; lower panel. Scale bar represents 10 μ m.

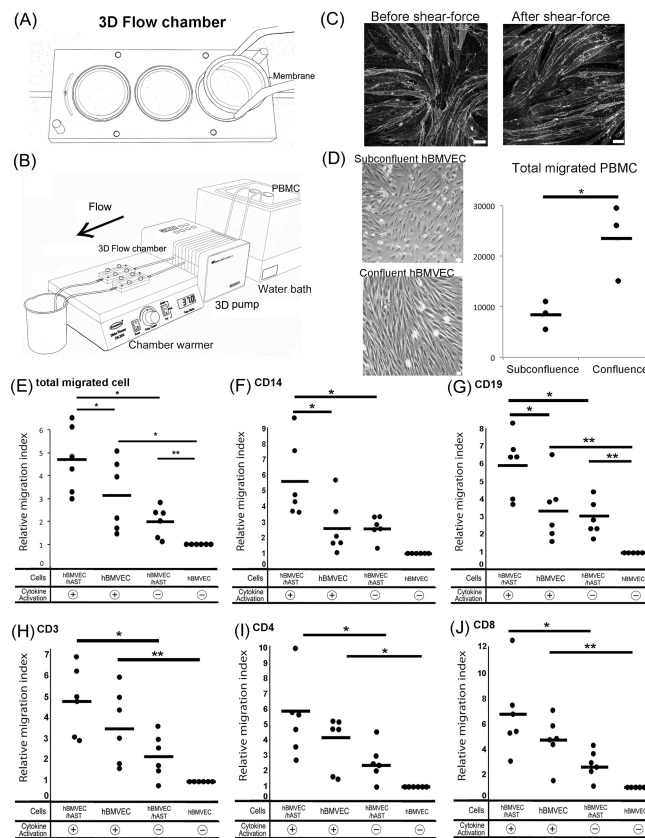


Fig. 5. Migration assay incorporating shear stress and membrane supported co-cultures. (A) Cartoon of 3D chamber and membrane. The chamber has three wells to accommodate membranes and two gateways for PBMC. (B) Cartoon of transmigration assay. With membranes in plate, chambers are connected to PBMC suspensions by silicon tubing. PBMC and chambers are kept in 37°C using water bath and chamber warmer. (C) Comparison of tight junction molecule before and after shear-force. Caludin-5 was detected in hBMVEC monoculture before (left panel) and after (right panel) transmigration. Subconfluent; 3×10^4 hBMVEC VS Confluent; 10×10^4 hBMVEC were seeded on the membrane at first day. They were mono-cultured for two days in 33°C and for one day in 37°C after activation. Image of subconfluent (D; upper panel) and confluent hBMVEC (D; lower panel). Comparison of total migrated cell number in subconfluent and confluent hBMVEC (D; left panel). Each symbol indicates one experiment. Effects of co-culture and activation on migrated cell numbers (E–J). Migrated cell number in each experiment was normalized to 1 using non activated hBMVEC/hAST and reported as relative migration index (RMI). * $P < 0.01$, ** $P < 0.05$